



ELSEVIER

Available online at www.sciencedirect.com

ScienceDirect

journal homepage: www.elsevier.com/locate/he

Mesoporous carbon as Pt support for PEM fuel cell

Federico A. Viva^a, Mariano M. Bruno^{a,b}, Esteban A. Franceschini^a,
Yohann R.J. Thomas^a, Guadalupe Ramos Sanchez^c, Omar Solorza-Feria^c,
Horacio R. Corti^{a,d,*}

^a Grupo Celdas de Combustible, Departamento de Física de la Materia Condensada, Centro Atómico Constituyentes, Comisión Nacional de Energía Atómica (CNEA), Av General Paz 1499, 1650 San Martín, Buenos Aires, Argentina

^b Escuela de Ciencia y Tecnología, Universidad de Gral. San Martín, Martín de Irigoyen 3100, 1650 San Martín, Buenos Aires, Argentina

^c Departamento de Química, Centro de Investigación y Estudios Avanzados del IPN, Av. IPN 2508, Col. San Pedro Zacatenco, A. Postal 14-740, 07360 Mexico D.F., Mexico

^d Instituto de Química Física de los Materiales, Medio Ambiente y Energía (INQUIMAE), Universidad de Buenos Aires – CONICET, Ciudad Universitaria, Pabellón II, 1428 Buenos Aires, Argentina

ARTICLE INFO

Article history:

Received 17 October 2013

Accepted 4 December 2013

Available online xxx

Keywords:

Mesoporous carbon

Supported Pt

ORR

RDE

Polarization curves

ABSTRACT

A mesoporous carbon (MP) supported Pt nanocatalyst was evaluated as anode and cathode catalyst for PEM fuel cell. Kinetics study of the oxygen reduction reaction were characterized by using the rotating disk electrode (RDE) and rotating ring disk electrode (RRDE) techniques in acid media. Membrane electrode assemblies (MEAs) were prepared using Pt supported on MP as anodic and cathodic catalysts and the fuel cell performance evaluated. Polarization and power curves show a similar performance as cathode catalyst when compared to commercial catalyst while there is an 8% improvement when used as anode catalyst.

Copyright © 2013, Hydrogen Energy Publications, LLC. Published by Elsevier Ltd. All rights reserved.

1. Introduction

The advantages of Polymer Exchange Membrane Fuel Cells (PEMFC) as portable and stationary power source have been widely described [1,2]. Nevertheless, PEMFC still struggle to position themselves in the market due that their efficiencies are not as high as the theoretical values and also due to manufacturing cost [3,4]. No catalyst other than Pt has been found yet to present a better catalytic efficiency, for the anode

and cathode reactions, which, due to its low natural abundance, possesses a high cost.

In relation with the previous statement, the support used for the metal catalyst nanoparticles plays a major role in the catalytic activity. It has been shown that the nature and morphology of the carbon support and the interaction between support and metal particles influences the nanoparticle dispersion on the support, the metal particles morphology, and the stability of the final catalyst [5–8], thus affecting the catalytic activity of the metal particles [9,10].

* Corresponding author. Grupo Celdas de Combustible, Departamento de Física de la Materia Condensada, Centro Atómico Constituyentes, Comisión Nacional de Energía Atómica (CNEA), Av General Paz 1499, 1650 San Martín, Buenos Aires, Argentina. Tel.: +54 11 6772 7174; fax: +54 11 6772 7121.

E-mail address: hrcorti@andar.cnea.gov.ar (H.R. Corti).

0360-3199/\$ – see front matter Copyright © 2013, Hydrogen Energy Publications, LLC. Published by Elsevier Ltd. All rights reserved.

<http://dx.doi.org/10.1016/j.ijhydene.2013.12.027>

Several ordered mesoporous carbons (OMC) with different synthesis conditions of drying, xerogels, cryogels and aerogels, and/or different casting conditions, hard and soft template, have been used as catalysts support for fuel cells [11,12]. These OMC possesses morphological properties such as surface area, pore sizes, surface groups, etc that have shown to improve the catalytic effect by an adequate metal nanoparticle size, nanoparticles distribution across the surface, anchoring of the nanoparticles to the support, and improvement of the reactant mass transport [13–15].

Recently our group has work in the preparation and characterization of metal nanoparticles catalyst on mesoporous carbon (MC) as fuel cell catalyst [15–18]. Pt catalyst supported on MC was used as cathode catalyst in direct methanol fuel cell (DMFC) showing improved results when compared against Pt supported on carbon Vulcan [18].

In the present work the Pt catalyst supported on MC, prepared by an impregnation and reduction method, was characterized by the rotating disk electrode (RDE) technique for the oxygen reduction reaction (ORR) and was employed as anode catalyst for the H₂ oxidation and cathode catalyst for the O₂ reduction. Fuel cell measurements were performed on 5 cm² active area single MEA cell and its performance compared against a commercial catalyst.

2. Experimental

2.1. Mesoporous carbon and catalyst supported preparation

Mesoporous carbon support was obtained using the method previously described [19]. Briefly, a precursor was prepared by polymerization of resorcinol (Fluka) and formaldehyde (Cicarelli, 37 wt %). Sodium Acetate (Cicarelli) was used as catalyst and a cationic polyelectrolyte (Polydiallyldimethylammonium chloride, PDADMAC, Sigma–Aldrich) was used as a structuring agent. The carbonized material at 1000 °C was grinded and passed through a mesh with a pore size of 40 μm. The mesoporous carbon has a surface area of 580 m² g⁻¹ as obtained by BET, and the pore size distribution shows a peak at 20 nm [19].

The preparation and characterization of Pt nanoparticles on MC was described elsewhere [17,18]. Briefly, adequate amounts of solutions of the metal precursors H₂PtCl₆·6H₂O (Tetrahedron) (Aldrich) was added to a slurry of the carbon support while stirring. The pH was adjusted to 8 with 1 M NaOH (Pro Analysis, Merck) aqueous solution and heated to 80 °C. NaBH₄ (granular 98%, Sigma Aldrich) was added in a molar ratio of 3:1 (NaBH₄ to metal salt) to the suspension while heating for 2 h, followed by stirring for 12 h at room temperature. The liquid was centrifuged and the solid was separated, washed and dried on a vacuum oven at 60 °C overnight. The obtained Pt/MC had a 35% metal loading with 3.1 mean particle diameter while for Pt/C the values were 38% and 4.2 nm, respectively, as obtained by thermogravimetric analysis (TG), X-ray diffraction (XRD) and transmission electron microscopy TEM [17].

2.2. Oxygen reduction analysis by RDE and RRDE

Oxygen reduction experiments were performed employing an Autolab PGSTAT302N potentiostat (Echochemie, Netherlands). For the rotating experiments the Autolab potentiostat was coupled to a Rotating Ring-Disk Electrode (RRDE, Pine Research Inst.; Raleigh, NC). A gold disk electrode (0.196 cm²) with platinum ring electrode (Pine Research Inst.) was used as the working electrode. A Saturated Calomel Electrode (SCE) was used as reference electrode and all potentials were referred to the Reference Hydrogen Electrode (RHE). The counter electrode was a large area rolled platinum wire (0.5 mm in diameter, 30 cm length). A three electrodes electrochemical cell with a jacket was employed, and its temperature was controlled by circulating a thermostated liquid using a Techne temperature controller. RDE and RRDE measurements were performed at 25 °C in 0.5 M H₂SO₄ aqueous media. Linear sweep Voltammograms (LSV) were recorded for the ORR at different rotation speed ($\omega = 100$ –2500 rpm). The potential was scanned between 1.0 and 2.0 V (vs. NHE) at 5 mV s⁻¹. The calibration of the RRDE was carried out by measuring the disk and ring currents in a 0.005 M K₃Fe(CN)₆ + 0.1 M K₂SO₄ electrolyte. The disk potential was cycled between 0.2 and 1.0 V at 5 mV s⁻¹ while the ring potential was fixed at 1.4 V in order to oxidize the Fe⁺³ generated in the disk. This procedure was repeated at different rotating speed. The RRDE collection efficiency (*N*) was determined from the slope of disc current (*I_D*) vs. ring current (*I_R*) plots [20–22].

2.3. MEA preparation and fuel cell testing

MEAs were prepared with Pt/MC on one electrode and commercial Pt/C 40% (E-TEK) on the other electrode. These MEAs were tested using the Pt/MC as anode and cathode catalyst. For comparison an MEA with commercial catalyst on both sides was also prepared. The catalyst was applied onto the membrane by spray method with an active area of 5 cm². The catalyst suspension was prepared by mixing the catalyst (0.5 mg Pt cm⁻²), with different amounts of Nafion solution (5% vol. Ion Power) and isopropanol. The Proton Exchange Membrane used was Nafion 117 (Ion Power) which was placed between two gas diffusion layers (Carbon Cloth 10% PTFE from ElectroChem Inc.) and pressed for 1.5 min at 120 °C with 100 kg cm⁻². The Nafion membrane was previously treated by boiling in H₂O₂ 3% (H₂O₂ 30%, Biopack) followed by H₂SO₄ 3% (95–97%, Merck). The MEAs were mounted in standard single cell housing with a serpentine flow fields. Proper Teflon gasket films (50–150 μm) were inserted and the cell uniformly bolted with a torque of 2.3 N m. O₂ and H₂ were humidified at 100% RH and fed to the cell, the humidifying bottles and the cell temperatures were controlled individually. After assembly of the cell, the MEA was subject to the following conditioning procedure. First, the temperatures were increased to values of 60 °C. Then the potential of the cell was maintained constant at 0.4 V for 25–30 min until the current stabilizes. The potential was then set back to open circuit voltage (OCV) until it remains constant and the polarization curve was registered. Those steps were repeated until no more change in the maximum power output was observed. Galvanodynamic polarization tests were performed at three different cell

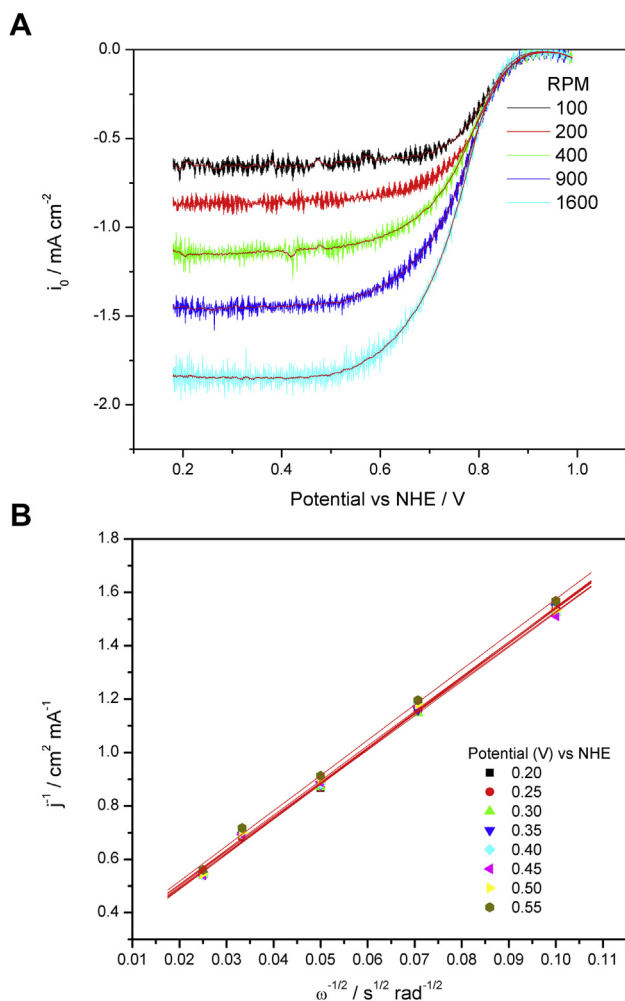


Fig. 1 – A) Linear sweep voltammetry curves obtained in 0.5 M H₂SO₄ for ORR for Pt/MC at different rotation rates. B) Koutecky–Levich plots showing the linear relation between j^{-1} and $\omega^{-1/2}$.

temperatures, 40, 60 and 80 °C with humidified H₂ and O₂ at a flow of 200 ml min⁻¹. Experiments were also conducted with back pressure control (30 psi) at the exit of the anode and cathode.

All fuel cell tests were performed with a Scribner fuel cell test station and in all cases the humidifier temperature was set 5 °C above the cell temperature.

3. Results and discussion

3.1. ORR analysis by RDE

The overall measured current density, j , of the oxygen reduction can be expressed in terms of the kinetic current density, j_k , and the diffusion limited current density, j_d , by the Koutecky–Levich (KL) equation [23]:

$$\frac{1}{j} = \frac{1}{j_k} + \frac{1}{j_d} = \frac{1}{j_k} + \frac{1}{B\omega^{1/2}} \quad (1)$$

B being,

$$B = 0.2nFC_0D_0^{2/3}\nu^{-1/6} \quad (2)$$

where 0.2 is a constant used when the rotation speed, ω , is expressed as rpm, n is the number of electrons transferred per molecule of O₂ reduced, F the Faraday constant, C_0 is the concentration of oxygen dissolved (1.1×10^{-6} mol cm⁻³), D_0 is the diffusion coefficient of oxygen in the solution (1.4×10^{-5} cm² s⁻¹) [24], and ν the kinematic viscosity of the 0.5 M H₂SO₄ solution (1.0×10^{-2} cm² s⁻¹) [24] all of them at 25 °C. It is possible to calculate the theoretical slope of the KL plot ($\log j$ vs. $\omega^{-1/2}$) considering a four electrons process, i.e., a complete reduction of O₂ to H₂O. The dependences of the oxygen concentration and diffusion coefficient with temperature were taken into account for corrections of the theoretical 4 electrons KL plots using the values presented in literature [25]. Fig. 1A shows a set of LSV obtained in an RDE configuration in O₂ saturated 0.5 M H₂SO₄ at 25 °C, which exhibit a well defined charge-transfer kinetic control, mixed kinetic-diffusion, and diffusion-limited currents. Fig. 1B shows the slopes of the KL plot from which the number of electrons involved in the ORR was calculated. The theoretical slope (considering $n = 4$) was 9.42 mA⁻¹ cm² rpm^{1/2} at 25 °C, while the experimental slope observed for Pt/MC was 12.9 mA⁻¹ cm² rpm^{1/2}. The measured KL slope yields $n = 3$ (considering a transfer coefficient $\alpha = 0.5$). Moreover, the determination of the number of electrons by KL for the Pt/C yield a value of 3.2 leading to the conclusion that the ORR follows the same mechanism for Pt/MC as for the commercial one. Tafel analysis was also performed at 25 °C in order to obtain information of the reduction mechanism in both, Pt/C and Pt/MC catalysts through the Tafel slope (b) and exchange current density (j_0). Usually, Tafel plots for the ORR on platinum electrodes show different well-defined slopes, at low and high current densities. In general, the slope at low current densities (related to the transfer of 2 electrons) is constant with temperature, and Tafel slopes are analyzed at high current densities (related to the transfer of 4 electrons). Fig. 2 shows the Tafel curves for Pt/MC and Pt/C. From the figure the values of b obtained were 119 mV dec⁻¹ for Pt/MC and 105 mV dec⁻¹ for Pt/C indicating that the rate determining step

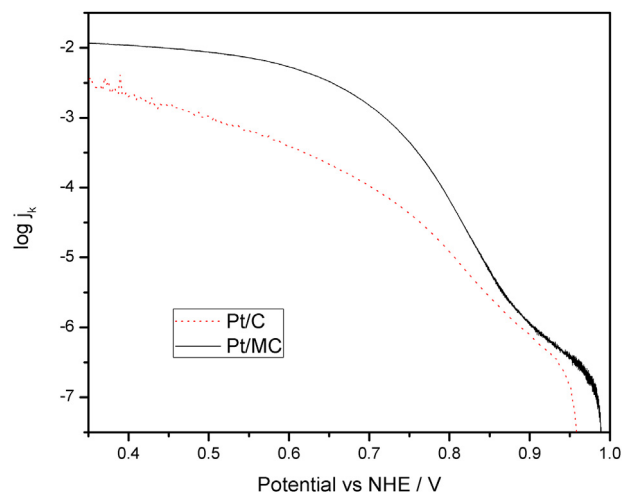


Fig. 2 – Tafel plots ($\log j$ vs potential) for Pt/C and Pt/MC.

(rds) for the ORR on both catalyst is the transfer of the first electron to the O_2 adsorbed onto the catalyst surface. This demonstrates that the ORR proceeds by the same mechanism on both catalysts as expected due that the carbon support should not modified the mechanism. From Fig. 2 can also be observed that the equilibrium potential (E_{eq}) for Pt/C is lower than for Pt/MC indicating that the overpotential needed in order to obtain a given current density would be lower for the last one. The exchange current, was evaluated taking into consideration the reversible oxygen electrode potential (E_r) at 25 °C [20,21]. The obtained values of j_0 for Pt/MC was $4.37 \times 10^{-5} \text{ mA cm}^{-2}$ and $5.79 \times 10^{-6} \text{ mA cm}^{-2}$ for Pt/C showing that Pt/MC presents higher catalytic activity than Pt/C, which is consistent with the observed difference in the E_{eq} .

3.2. ORR analysis by RRDE

The RRDE analysis allows us to calculate the H_2O_2 percentage generated during the O_2 reduction using the equation [26]:

$$\%H_2O_2 = \frac{200I_R/N}{I_D + I_R/N} \quad (3)$$

where N is the experimental collection efficiency which corresponds to the I_R/I_D ratio ($N = 0.18$). Percentages of H_2O_2 vs. cell potential at different rotation speeds were calculated using Eqn. (3), and they are shown in Fig. 3. For Pt/MC a maximum value of 0.25% at 200 rpm and 0.9 at 900 rpm were obtained. This result indicates that, at 25 °C, the ORR proceeds mostly to water, with a yield of ~99%, following preferentially a 4 electron transfer reaction mechanism. However, although the production of H_2O_2 is low, is not negligible and presents a dependence on the applied potential. On the other hand, the percentage of H_2O_2 for Pt/C are 1.25% (200 rpm) and 2% (900 rpm) being the amount of H_2O_2 formed 2 to 3 times higher than those obtained for Pt/MC.

3.3. Fuel cell test

Polarization measurements at the three different temperatures for the Pt/MC as anode and cathode catalyst with a

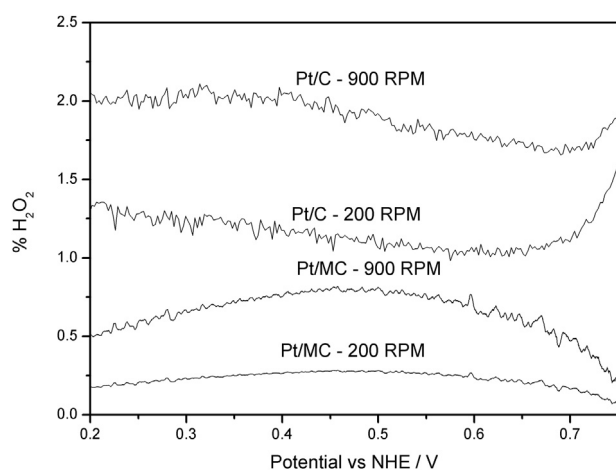


Fig. 3 – Percentage of H_2O_2 produced as function of the disk potential at different rotating rates at 25 °C.

backpressure of 30 PSI are shown in Fig. 4(A, B). As anode catalyst, Pt/MC shows high limiting current density (j_{lim}) and peak power densities (P_{peak}), attaining ca. 300 mW cm^{-2} at 80 °C. As cathode catalyst, the Pt/MC shows a good overall performance only at 80 °C presenting high j_{lim} and a P_{peak} of 260 mA cm^{-2} .

Fig. 5 shows the comparison of Pt/MC as anode and cathode catalyst against an MEA prepared with commercial Pt/C on both electrodes at 80 °C and 30 PSI back pressure. From Fig. 5 can be observed that the j values in the polarization are higher for the commercial catalyst up to a value of 400 mA cm^{-2} . Above that value, j decreases sharply than for the Pt/MC as anode and cathode catalyst. The limiting current is 200 mA cm^{-2} and 300 mA cm^{-2} higher for Pt/MC as cathode and anode respectively than for Pt/C. The P_{peak} density is ca 5% lower for Pt/MC that for Pt/C. On the other hand, P_{peak} for Pt/MC as anode catalyst is 8% higher than Pt/C. A closer look at the polarization curves indicates that the mass transport is better on the MEA that uses Pt/MC as catalyst when compared to the one prepared with commercial ones. This is observed at the high current density zone of the polarization plot, where the mass transport overpotential controls the polarization. As indicated above the polarization decreases sharply above a

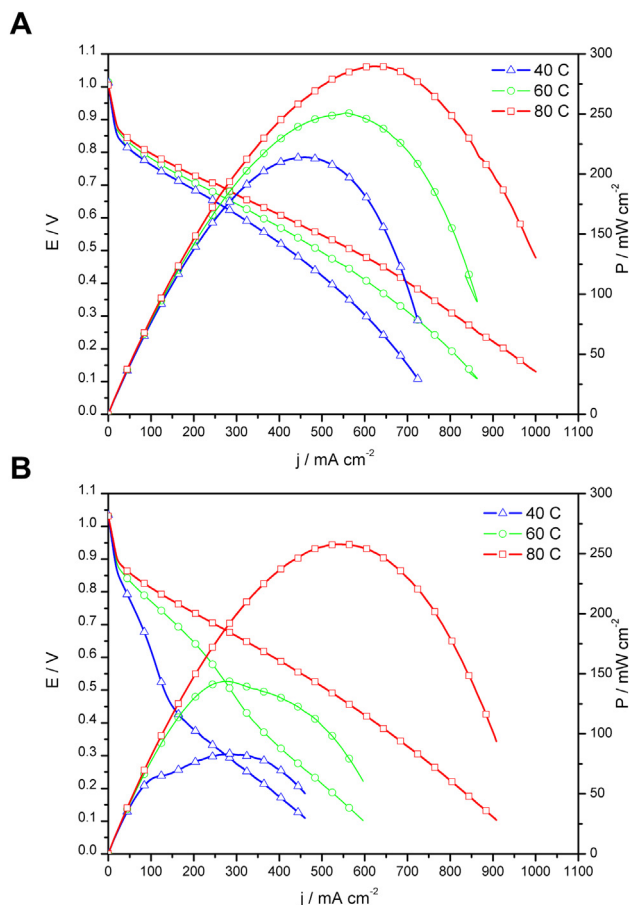


Fig. 4 – Polarization and power plots at different temperatures for MEAs prepared with A) Pt/MC as anode catalyst. B) Pt/MC as cathode catalyst. In all cases commercial Pt/C was used in opposite electrode and 30 PSI back pressure at the anode and cathode.

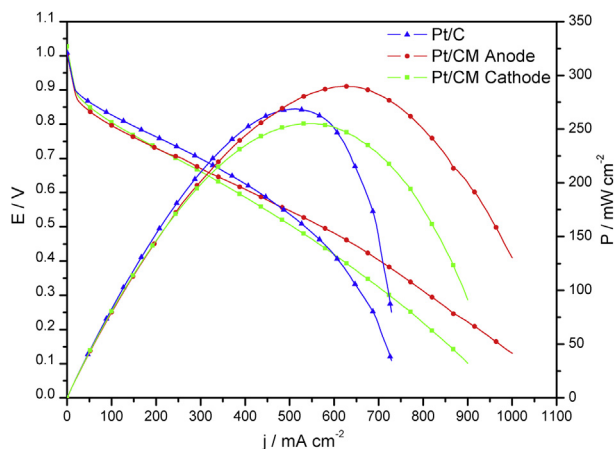


Fig. 5 – Polarization and power plots for Pt/MC as anode and as cathode catalyst vs the commercial catalyst at 80 C and 30 PSI back pressure.

current density of 400 mA cm^{-2} for Pt/C while that is not the case for Pt/MC as anode or cathode catalyst. Similar results were observed in previous works where PtRu was deposited on MC and used as anode catalyst for DMFC [15,17], and also as support for PdNi₂ catalyst for cathodes of DMFC [16]. In those reports, it was shown that the MC not only provide a suitable substrate that resulted in a highly dispersed catalyst with a narrow particle size distribution, but also the mass transport showed improvements when compared to the catalyst supported on Vulcan carbon.

In Sections 3.1 and 3.2 was shown that Pt/MC catalyst presents a better catalytic activity towards ORR than Pt/C. However, the results described above showed a lower power for Pt/MC as cathode catalyst than for Pt/C even though the mass transport controlled region is better. Different factors affect the overall performance of the fuel cell besides the catalyst catalytic activity, such as catalyst deposition method, catalyst ink formulation and pressing conditions to name a few. Moreover, the hydrophilicity/hydrophobicity in the anode and cathode might be different depending on the material composition and test conditions. In order to further evaluate the role of the MC, MEAs with different formulation in terms of the amount of Nafion binder used in the ink of the cathode side were evaluated. The different MEAs with an amount of Nafion binder, by weight of the final catalyst deposited on the gas diffusion layer, from 10% to 50% were measured at 80 °C and 30 PSI BP. Polarization of those MEAs rendered curves similar to the one showed in Fig. 5B for 80 °C. Fig. 6 shows the normalized P_{peak} obtained with the different concentration of Nafion binder in the cathode. Can be observed from the figure, that with 35% w/w of Nafion there is a maximum of the P_{peak} obtained. Rao et al. [27] demonstrated that the material porosity have a crucial effect in the catalyst participation on the triple phase boundary. Nafion penetration in small pores (<20 nm) is hindered, reducing therefore the formation of the triple phase boundary. Thus, the results might be explained by the improvement of the triple phase boundary by improving the ionic contact with the catalyst surface [28].

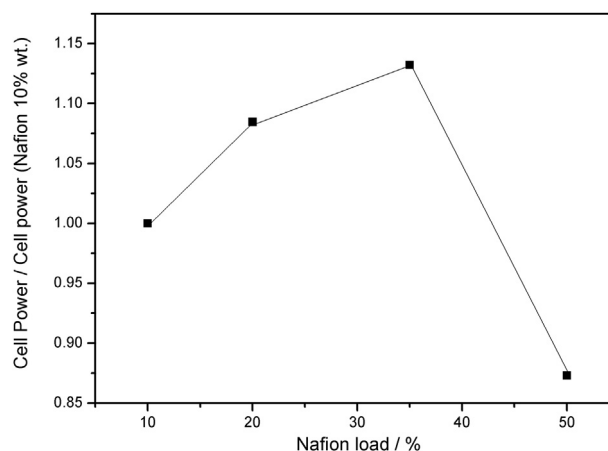


Fig. 6 – P_{peak} for the different amounts of Nafion used in the final catalyst for Pt/MC used as cathode catalyst.

4. Conclusions

The effect of a mesoporous carbon support on the catalytic performance of Pt nanoparticles was analyzed. The catalyst prepared was evaluated for hydrogen oxidation reaction and oxygen reduction reaction. Mesoporous carbon with a pore distribution of about 20 nm and a pore volume of $0.99 \text{ cm}^3 \text{ g}^{-1}$ was chosen as support. The Pt nanoparticles were obtained by the impregnation method by sodium borohydride reduction in aqueous media.

The supported catalyst was characterized by RDE and RRDE for ORR. The catalyst support on MC showed a lower overpotential than Pt supported on Vulcan to achieve similar current density in Tafel plot. Moreover, Pt/MC has lesser peroxide generation performance. However, the mesoporous support although presents a positive effect in the mass transports does not shows a significant positive effect on the power density. The Pt/MC showed better cell performance than Pt/C as anode catalyst. Pt/MC catalyst in the anode section showed a P_{peak} 8% higher than Pt/C. Furthermore, at high current densities the Pt/MC showed better mass transport, demonstrating a positive effect of the mesoporosity of carbonous support in the performance of catalyst layer. Porous carbon with mesopores around 20 nm has positive effect on mass transport in cell performance. However, there is still a lacking in works evaluating the optimum conditions of mesoporous support in a fuel cell, where the effects of the preparation of the catalytic layer are crucial. This different result would indicate that the MC is promising for catalyst support in fuel cells, a forthcoming work analyzing in detail the optimum conditions for the formulation of catalytic ink in a catalyst layer will be presented.

Acknowledgments

The authors thank financial support from bilateral project México-Argentina, CONACYT-MINCYT 2008–2010, CONACYT (México) and ANPCyT (Argentina, PICT 35403 and 008 PRH 200-4). EF and YRJT thanks CONICET and GRS thanks CONACYT for

their doctoral fellowship. FAV, MMB and HRC are permanent research fellows of CONICET.

REFERENCES

- [1] Peighambardoust SJ, Rowshanzamir S, Amjadi M. Review of the proton exchange membranes for fuel cell applications. *Int J Hydrogen Energy* 2010;35:9349–84.
- [2] Kriston Á, Xie T, Gamliel D, Ganesan P, Popov BN. Effect of ultra-low Pt loading on mass activity of polymer electrolyte membrane fuel cells. *J Power Sources* 2013;243:958–63.
- [3] Bar-on I, Kirchain R, Roth R. Technical cost analysis for PEM fuel cells. *J Power Sources* 2004;109(2002):71–5.
- [4] O'Hayre R, Cha SW, Colella W, Prinz FB. *Fuel cell fundamentals*. New York: John Wiley & Sons; 2006.
- [5] Figueiredo J, Pereira M, Serp P, Kalck P, Samant P, Fernandes J. Development of carbon nanotube and carbon xerogel supported catalysts for the electro-oxidation of methanol in fuel cells. *Carbon* 2006;44:2516–22.
- [6] Liu H, Song C, Zhang L, Zhang J, Wang H, Wilkinson D. A review of anode catalysis in the direct methanol fuel cell. *J Power Sources* 2006;155:95–110.
- [7] Cui Z, Liu C, Liao J, Xing W. Highly active PtRu catalysts supported on carbon nanotubes prepared by modified impregnation method for methanol electro-oxidation. *Electrochim Acta* 2008;53:7807–11.
- [8] Park SJ, Kim BJ, Lee SY. Effect of surface modification of mesoporous carbon supports on the electrochemical activity of fuel cells. *J Coll Interfac Sci* 2013;405:150–6.
- [9] Arbizzani C, Beninati S, Soavi F, Varzi a, Mastragostino M. Supported PtRu on mesoporous carbons for direct methanol fuel cells. *J Power Sources* 2008;185:615–20.
- [10] Alegre C, Calvillo L, Moliner R, Gonzalez-Exposito JA, Guillen-Villafuerte O, Martinez Huerta MV, et al. Pt and PtRu electrocatalysts supported on carbon xerogels for direct methanol fuel cells. *J Power Sources* 2011;196:4226–35.
- [11] Joo SH, Pak C, You DJ, Lee S-A, Lee HI, Kim JM, et al. Ordered mesoporous carbons (OMC) as supports of electrocatalysts for direct methanol fuel cells (DMFC): effect of carbon precursors of OMC on DMFC performances. *Electrochim Acta* 2006;52:1618–26.
- [12] Sharma S, Pollet BG. Support materials for PEMFC and DMFC electrocatalysts – a review. *J Power Sources* 2012;208(0):96–119.
- [13] Joo SH, Kwon K, You DJ, Pak C, Chang H, Kim JM. Preparation of high loading Pt nanoparticles on ordered mesoporous carbon with a controlled Pt size and its effects on oxygen reduction and methanol oxidation reactions. *Electrochim Acta* 2009;54:5746–53.
- [14] Cheon JY, Ahn C, You DJ, Pak C, Hur SH, Kim J, et al. Ordered mesoporous carbon-carbon nanotube nanocomposites as highly conductive and durable cathode catalyst supports for polymer electrolyte fuel cells. *J Mater Chem A* 2013;1:1270–83.
- [15] Bruno MM, Petrucci MA, Viva FA, Corti HR. Mesoporous carbon supported PtRu as anode catalyst for direct methanol fuel cell: polarization measurements and electrochemical impedance analysis of mass transport. *Int J Hydrogen Energy* 2013;38:4116–23.
- [16] Ramos-Sánchez G, Bruno MM, Thomas YRJ, Corti HR, Solorza-Feria O. Mesoporous carbon supported nanoparticulated PdNi₂: a methanol tolerant oxygen reduction electrocatalyst. *Int J Hydrogen Energy* 2012;37:31–40.
- [17] Viva FA, Bruno MM, Jobbagy M, Corti HR. Electrochemical characterization of PtRu nanoparticles supported on mesoporous carbon for methanol electrooxidation. *J Phys Chem C* 2012;116:4097–104.
- [18] Bruno MM, Viva FA, Petrucci MA, Corti HR. Pt electrocatalyst supported on mesoporous carbon as cathode for direct methanol fuel cell. *J Appl Elect* 2013 [submitted for publication].
- [19] Bruno MM, Cotella NG, Miras MC, Koch T, Seidler S, Barbero C. Characterization of monolithic porous carbon prepared from resorcinol/formaldehyde gels with cationic surfactant. *Colloids Surfaces A* 2010;358:13–20.
- [20] Suárez-Alcántara K, Rodríguez-Castellanos a, Dante R, Solorza-Feria O. RuxCrySez electrocatalyst for oxygen reduction in a polymer electrolyte membrane fuel cell. *J Power Sources* 2006;157:114–20.
- [21] Suárez-Alcántara K, Solorza-Feria O. Evaluation of RuxWySez catalyst as a cathode electrode in a polymer electrolyte membrane fuel cell. *Fuel Cells* 2010;10:84–92.
- [22] Franceschini EA, Bruno MM, Viva F a, Williams FJ, Jobbágy M, Corti HR. Mesoporous Pt electrocatalyst for methanol tolerant cathodes of DMFC. *Electrochim Acta* 2012;71:173–80.
- [23] Bard AJ, Faulkner LR. *Electrochemical methods. Fundamentals and applications*. 1st ed. J. Wiley & Sons; 1980.
- [24] Coutanceau C, Crouigneau P, Léger JM, Lamy C. Mechanism of oxygen electroreduction at polypyrrole electrodes modified by cobalt phthalocyanine. *J Electroanal Chem* 1994:389.
- [25] Lide DR. *CRC handbook of chemistry and physics*. 90th ed. CRC; 2009.
- [26] Gasteiger HA, Gu W, Makharia R, Mathias MF, Sompalli B. In: Vielstich W, Lamm A, Gasteiger HA, editors. *Handbook of fuel cells: fundamentals, technology, applications*. West Sussex, UK: John Wiley & Sons; 2003.
- [27] Rao V, Simonov PA, Savinova ER, Plaksin GV, Cherepanova SV, Kryukova GN, et al. The influence of carbon support porosity on the activity of PtRu/Sibunit anode catalysts for methanol oxidation. *J Power Sources* 2005;145:178–87.
- [28] Mu S, Tian M. Optimization of perfluorosulfonic acid ionomer loadings in catalyst layers of proton exchange membrane fuel cells. *Electrochim Acta* 2012;60:437–42.